

**Connectivity in the cold: the comparative population genetics of vent-endemic fauna in the
Scotia Sea, Southern Ocean.**

C.N. Roterman^{a*}, J.T. Copley^b, K.T. Linse^c, P.A. Tyler^b, A.D. Rogers^a

^a Department of Zoology, University of Oxford, South Parks Road, Oxford, OX1 3PS, UK

^b Ocean and Earth Science, University of Southampton, Waterfront Campus, Southampton,
SO14 3ZH, UK

^c British Antarctic Survey, High Cross, Madingley Road, Cambridge, CB3 0ET, UK

* Corresponding author: christopher.roterman@zoo.ox.ac.uk

Keywords: Hydrothermal Vents, Southern Ocean, *Kiwa*, *Gigantopelta*, *Lepetodrilus*, Connectivity

Running Title: Connectivity of vent-endemic fauna in the Scotia Sea

Abstract

We report the first comparative population genetics study for vent fauna in the Southern Ocean using cytochrome C oxidase I and microsatellite markers. Three species are examined: the kiwaid squat lobster, *Kiwa tyleri*, the peltospirid gastropod *Gigantopelta chessoia* and a lepetodrilid limpet, *Lepetodrilus* sp. collected from vent fields 440 km apart on the East Scotia Ridge (ESR) and from the Kemp Caldera on the South Sandwich Island Arc, ~95 km eastwards. We report no differentiation for all species across the ESR, consistent with panmixia or recent range expansions. A lack of differentiation is notable for *Kiwa tyleri*, which exhibits extremely abbreviated lecithotrophic larval development, suggestive of a very limited dispersal range. Larval lifespans may, however, be extended by low temperature-induced metabolic rate reduction in the Southern Ocean, muting the impact of dispersal strategy on patterns of population structure. COI diversity patterns suggest all species experienced demographic bottlenecks or selective sweeps in the past million years and possibly at different times. ESR and Kemp limpets are divergent, although with evidence of very recent ESR-Kemp immigration. Their divergence, possibility indicative of incipient speciation, along with the absence of the other two species at Kemp, may be the consequence of differing dispersal capabilities across a ~1000 m depth range and/or different selective regimes between the two areas. Estimates of historic and recent limpet gene flow between the ESR and Kemp are consistent with predominantly easterly currents in the region and potentially therefore, cross-axis currents on the ESR, with biogeographic implications for the region.

Introduction

Hydrothermal vents host colossal densities of macrofauna sustained by chemosynthetic bacteria, which is in stark contrast with the majority of the deep-sea floor where food is extremely limited (Gage & Tyler 1992). Vent fields, which are found on mid-ocean ridges (MORS), back-arc spreading basins and volcanically active seamounts, can be conceived of as habitat patches, separated by tens to hundreds of kilometres of deep-sea floor. Such patches are considered ephemeral, lasting decades to millennia, as geothermal heat sources are disrupted by plate tectonic movements and eruptions can suddenly resurface fields with fresh basalt (Van Dover 2000).

This habitat patchiness and ephemerality necessitates the maintenance of vent metapopulations by larval dispersal between fields, making vent fauna ideal candidates for examining the way realised larval dispersal affects genetic connectivity and diversity in benthic marine metapopulations in general (Jollivet *et al.* 1999; Vrijenhoek 1997; 2010). Despite this common requirement, there is a surprising diversity of dispersal strategies, which appears phylogenetically constrained (Tyler & Young 2003). The historical paradigm has held that lecithotrophic larvae have a more limited dispersal range compared to planktotrophic larvae as their planktonic larval duration (PLD) is limited by the size of their nutritional reserves (Jablonski & Lutz 1983). The evidence for a correlation between dispersal strategy, PLD, species range and population structure in the marine environment and particularly in the deep sea (both at vents and in general), however, is equivocal (Creasey & Rogers 1999; Weersing & Toonen 2009; Vrijenhoek 2010; Selkoe & Toonen 2011; Faurby & Barber 2012; Mercier *et al.* 2013). Dispersal strategy may therefore be unreliable as a predictor of species range and patterns of population structure, with other factors (e.g. temperature, hydrography, habitat patchiness and sea floor topography) having an equal or greater impact. For example, vent fauna producing planktotrophic larvae have yet to be reported from polar regions (Pedersen *et al.* 2010; Rogers *et al.*

2012; Hahm *et al.* 2015) and it has been suggested this is the consequence of the extreme seasonality of food supply in high latitude surface waters (Pearse *et al.* 1991; Rogers *et al.* 2012).

The same factors affecting population structure will also affect the genetic diversity of vent metapopulations. Greater site occupancy and lower vent field ephemerality along a ridge should result in higher levels of genetic diversity, owing to a reduced likelihood of demographic bottlenecks; a pattern observed on the East Pacific Rise (EPR) (Vrijenhoek 2010). The near ubiquitous presence of star-like mtDNA haplotype networks (and negative Tajima's *D*, Fu's *F_s*) amongst vent-endemic fauna, consistent with recent demographic expansions following bottlenecks, likely reflects the general state of demographic instability of vent metapopulations subject to stochastic changes in site occupancy along MORs (e.g. Plouviez *et al.* 2009; 2013; Teixeira *et al.* 2010).

Since the discovery of vents in 1977 (Corliss *et al.* 1979), the East Pacific has been the focus of population genetics studies (summarised by Vrijenhoek 2010) but more recently, research has extended to other areas in the Pacific, Atlantic, Indian and Southern oceans (Thaler *et al.* 2011; Teixeira *et al.* 2012; Chen *et al.* 2015a; c). Few studies, however, involve multiple species comparisons (Plouviez *et al.* 2009; Thaler *et al.* 2014), which can provide insights into the ways life history traits affect vent-endemic populations in the face of present and past geophysical conditions. In this study we report the first multi-species population genetics data for vent fauna in the Southern Ocean, featuring the entire known distribution range of three recently discovered species in the Scotia Sea: the kiwaid squat lobster, *Kiwa tyleri* (Thatje *et al.* 2015a), the peltospirid gastropod, *Gigantopelta chessoia* (Chen *et al.* 2015c) and a lepetodrilid limpet, *Lepetodrilus* sp.

Setting

The East Scotia Ridge (ESR) is an isolated back-arc spreading ridge, which is divided into nine segments (E1-E9) and spans ~500 km in the Scotia Sea (Fig. 1A). Black smoker hydrothermal venting, hosting dense assemblages of macrofaunal species has been observed on the E2 and E9 segments, which are ~440 km apart (Rogers *et al.* 2012). These two segments are characterized by shallow (~2500 m depth), axial highs (Fig. 1B) indicating the presence of underlying buoyant magma plumes related to their proximity to the subducting South American plate (Baker *et al.* 2005; Livermore 2006). In contrast, Segments E3-E9 have deep (~3500-4500 m depth) axial valleys indicating an absence of such magmatic plumes. The presence of confirmed venting only at the topographical highs of the E2 and E9 segments may indicate that venting is largely restricted to such shallow sites and is rare on other ridge segments, although the signature of a hydrothermal plume has been detected over the shallowest portion of the E5 segment (Baker *et al.* 2005; Livermore 2006). Consequently, dispersal stepping stones between E2 and E9, may be few and far between for vent-endemic fauna.

Only 95 km to the east of E9 are shallower vents (~1,400 m depth) recently discovered within the Kemp Caldera (herein referred to as Kemp), part of the South Sandwich Island (SSI) volcanic back-arc system (Rogers 2010) (Fig. 1A). These vents are situated on a volcanic sub-cone within a 7km-wide caldera, the rim of which rises to ~800 m depth, potentially isolating their inhabitants from ocean currents (Fig. 1C). Observations of ash and sulphur deposits (Rogers 2010) and extremely high [H₂S] in the vent fluid (~200 mM) indicate a very recent volcanic ‘blow-out’ event occurred (Cole *et al.* 2014). Sulphur-coated white smoker chimneys were largely devoid of fauna and of the three study species, only *Lepetodrilus* sp. was found on hard substrata adjacent to the venting, with the other two study species being absent.

The easterly-flowing Antarctic Circumpolar Current (ACC) dominates the current regime of the Southern Ocean. Within the Scotia Sea, cold bottom waters (< 0 °C) around the ESR and SSI are a mix

of Weddell Sea Deep Water and variants of Circumpolar Deep Water, generally flowing east or north-easterly (Fig. 1) (Orsi *et al.* 1999; Naveira-Garabato *et al.* 2002; Meredith *et al.* 2008). Strong, cross-axis currents have been measured on the E9 segment, consistent with this picture (Larter 2009). The possible combination of few dispersal stepping stones with cross-axis currents along portions of the ESR could limit connectivity along the ESR to a greater extent than equivalent distances along other ridges.

Study species

The study species were chosen on the grounds of being the most visually and numerically dominant immediately adjacent to venting chimneys. On the ESR, kiwaid ‘crabs’ were observed closest to venting fluid on the sides and bases of chimneys (Rogers *et al.* 2012) at densities exceeding 700 m⁻² (Marsh *et al.* 2012). These anomuran crustaceans belong to a recently discovered family of chirostyloid squat lobsters found only in deep-sea chemosynthetic ecosystems (Macpherson *et al.* 2005; Schnabel & Ahyong 2011; Roterman *et al.* 2013b). The dorsal surface of *Kiwa tyleri* features a dense covering of hair-like setae supporting chemosynthetic microbial episymbionts, which appears to be their principle source of nutrition (Reid *et al.* 2013; Thatje *et al.* 2015a). *Kiwa tyleri* females produce few (~200), but very large (~1800 µm diameter) eggs, which are likely brooded for an extended period (> 18 months) (Marsh *et al.* 2015). Freshly hatched zoea larvae resemble functional, non-buoyant, non-swimming megalopa, with large yolk reserves sufficient for extended food-independent development (> 1 year) (Thatje *et al.* 2015b). *Kiwa tyleri* appears therefore to exhibit the most abbreviated development known amongst crab-like decapods, (Thatje *et al.* 2015b); suggesting a reproductive strategy geared towards high maternal investment in offspring and larval retention close to the natal site (Marsh *et al.* 2015; Thatje *et al.* 2015b). Owing to the inability of reptant decapods to down-regulate [Mg²⁺] in temperatures approaching 0 °C resulting in narcotization (Frederich *et al.*

2001), individuals may be restricted to a narrow thermal envelope around the vent effluent, preventing the dispersal of adults (Thatje *et al.* 2015a).

Next to the kiwaid assemblage on the ESR vents at densities exceeding 1500 m⁻², were large peltospirid gastropods *Gigantopelta chessoia*, which along with *G. aegis* and the scaly-foot gastropod *Chrysomallon squamiferum* are the only known gastropods to house endosymbiotic bacteria in an enlarged oesophageal gland (Chen *et al.* 2015b; c). Little is presently known of their life history, but their protoconch morphology is consistent with lecithotrophic dispersal (Chen *et al.* 2015c), as are examinations of East Pacific peltospirid oocytes (Tyler *et al.* 2008; Matabos & Thiebaut 2010).

Lepetodrilus sp. limpets were the most numerous of the study species (> 50,000 m⁻² at E9; Leigh Marsh, personal communication) and found at all three sites apparently grazing on the microbial films growing adjacent to vent effluent. Lepetodrilid limpets are commonly found at hydrothermal vents and sometimes also at other chemosynthetic habitats such as hydrocarbon seeps and whale carcasses (Johnson *et al.* 2008; Amon *et al.* 2013), making them potentially the most habitat flexible of the study species. Unlike those on the ESR, the Kemp limpets exhibited evidence of shell corrosion (Katrin Linse, personal communication). *Lepetodrilus* spp. females produce numerous (up to ~1,800) small (< 90 µm diameter), actively swimming lecithotrophic larvae (Lutz *et al.* 1986; Tyler *et al.* 2008). Both lepetodrilid and peltospirid larvae have been found in the buoyant hydrothermal plume and close to the seafloor around vents in the Pacific, indicating a capacity for long-range dispersal along currents entrained by ridge axes (Mullineaux *et al.* 1995; 2005).

Aims and Expectations

This study, characterises the population genetics of the three study species at hydrothermal vents in the Scotia Sea using mitochondrial sequences and custom-designed microsatellite markers. It provides

an opportunity to examine the patterns of population structure, gene flow and genetic diversity of fauna inhabiting hot vents surrounded by frigid water. Based on what is known about the dispersal strategies of the three species, it was expected that *Kiwa tyleri* would exhibit population structure along the ESR, owing to its extremely abbreviated larval development, whereas the two gastropod species would be less likely to exhibit structure. The limpets at Kemp were expected to be divergent from those on the ESR (and with a smaller effective population size), owing to the presumed topographical isolation of the caldera; with the historical direction of gene flow reflecting the predominantly west-to-east current regime. As is the case for nearly all vent-endemic fauna, the three species were expected to exhibit evidence of demographic change associated with the inherent demographic instability of vent metapopulations.

Materials and Methods

Sampling and DNA Extraction

Aggregations of macrofauna were sampled with a ‘slurp gun’ from the sides and bases of chimneys using the remotely operated vehicle *ISIS*, which was deployed from the Royal Research Ship *James Cook* during the JC042 expedition (Rogers 2010) (Table 1, Fig. 1). The chimneys sampled at E2 were ~30 m apart and those at E9, ~450 m apart. All individuals within a sample were collected from the same location within a few metre of each other. Fresh tissue (gastropod foot and kiwaid pereopod muscle) was excised, placed in Corning® 5 ml cryotubes in 96% ethanol and stored at -20 °C. Total genomic DNA was extracted from the tissue using the Qiagen DNeasy® Blood and Tissue Kit (Cat. 69506).

COI Sequencing and Analyses

PCR Reactions were performed in 9 μ l volumes on a Bio-Rad C1000 Thermal Cycler containing 0.6 μ l of each primer (forward and reverse) at a concentration of 4 pmol/ μ l, 6 μ l of Qiagen HotStarTaq Master Mix, 1.5 μ l of DNA template (~50-100 ng/ μ l) and 0.3 μ l of double-distilled water. Universal invertebrate primers, LCO1490 and HCO2198 (Folmer *et al.* 1994) were used to amplify COI from *K. tyleri* and *G. chessoia*, yielding fragments ~500 bp in length. For *G. chessoia*, this dataset is an augmentation of a smaller dataset of sequences in Chen *et al.* (2015c). For *Lepetodrilus* sp., new specific primers, LepESR-F (5'-TAACGATATGCGTTGACCATT-3') and LepESR-R (5'-ACCCGGGAAGAATCAGAATA-3') were designed using a COI fragment template generated by Leese *et al.* (2012). This primer may be effective with other members of the genus. All PCR reactions were performed as follows: initial HotStarTaq denaturation at 95 °C for 15 minutes, followed by 40 cycles of 94 °C for 45 seconds, 50 °C for 1 minute, 72 °C for 1 minute and a final extension of 5 minute at 72 °C. Sequences were deposited in Genbank (Acc# KU312406 - KU312689).

Descriptive diversity statistics as well as pairwise F_{ST} values indicating the degree of genetic differentiation between sample sites (10^5 permutations) were calculated in Arlequin 3.5.1.3 (Excoffier & Lischer 2010). To test for demographic history, Fu's F_s test (Fu 1996) and mismatch distributions assessed with Harpending's raggedness index (Hri) (Rogers & Harpending 1992), both with 10^4 bootstrap replicates, were implemented in Arlequin. Median-Joining networks, representing the most parsimonious relationships between haplotypes were calculated using Network 4.6.1.1 (Bandelt *et al.* 1999).

To date possible genetic bottlenecks, Bayesian Skyline Plots (BSPs) reconstructing demographic histories based on inferred genealogies to the coalescent (Ho & Shapiro 2011), were generated in Beast 1.8.2 (Drummond & Rambaut 2007) for populations as defined by F_{ST} . All analyses ran for 10^7 Markov Chain Monte Carlo (MCMC) generations with 10% discarded as 'burn-in'. Genealogies and model parameters were sampled every thousand generations and analyses were replicated twice to

ensure consistent results. Both runs were then combined using LogCombiner 1.8.2 (Drummond & Rambaut 2007) to estimate parameters. The model of evolution for each population was chosen with PartitionFinder (Lanfear *et al.* 2012), using both the Akaike information criterion (AIC) and the more conservative Bayesian information criterion (BIC) (Minin *et al.* 2003). Both criteria favoured the Tamura-Nei model with invariant sites for all three species as well as gamma-distributed rate variation among sites for the kiwaidids.

BSP runs were calibrated with taxon-centric COI substitution rates generated from the divergence of vent-associated geminate species either side of the Easter Microplate on the Southern East Pacific Rise (SEPR) under a strict molecular clock model. The microplate formed ~5.25-2.47 Ma (Naar & Hey 1991; Rusby & Searle 1995), with a mean age of 3.86 Ma. For *K. tyleri*, the 7.3% divergence of *Bythograea* spp. brachyuran crabs (Guinot & Hurtado 2003) gave a rate of 9.45596×10^{-9} substitutions/locus/year. For *G. chessoia*, a neomphaline gastropod-specific substitution rate of 1.45078×10^{-8} was estimated based on the 11.2% divergence of *Pachydermia* spp. (Matabos *et al.* 2011) and for the limpet, a *Lepetodrilus*-specific rate of 1.0583×10^{-8} was used based on the 8.17% divergence of the *L. pustulosus* species complex (Johnson *et al.* 2008). BSP reconstructions were visualised in TRACER 1.5 (Rambaut & Drummond 2007).

Microsatellite Genotyping and Analyses

Microsatellite markers developed by Roterman *et al.* (2013a) were used in this study: nine loci for *K. tyleri*, 12 loci for *G. chessoia* and 14 loci for *Lepetodrilus* sp.. All loci were amplified in singleplex reactions with 6-Fam tagged forward primers as per PCR protocols in Roterman *et al.* (2013a). Size-fragment analyses of the PCR products were conducted on an ABI 3730xl DNA analyser. Chromatograms were scored using Peak Scanner 1.0. Genotyping error rates were calculated by comparing 24 individuals with those same individuals genotyped in Roterman *et al.* (2013a). Diversity

statistics as well as tests for deviation from Hardy-Weinberg Equilibrium (HWE) and linkage disequilibrium (LD) were generated with Arlequin and corrected for multiple comparisons using the sequential Bonferroni approach (Rice 1989). Allelic richness was calculated with Fstat 2.9.3.2 (Goudet 1995). LD was examined with a likelihood ratio test (10^4 permutations) and an exact test of HWE was performed (10^6 Markov chain steps and 10^6 dememorisation steps). Presence of null alleles, excessive stutter and large allele dropout were assessed using MicroChecker (10^3 randomisations) (van Oosterhout *et al.* 2004). Loci were screened using LOSITAN (Antao *et al.* 2008) to test for the potential influence of selection by an F_{ST} outlier method (Beaumont & Nichols 1996). 10^6 simulations were performed, with the Infinite Alleles mutational Model (IAM) as well as the Stepwise Mutational Model (SMM). Significance was set at the 95% confidence level with a false discovery rate of 0.1. Microsatellite markers showing deviations from HWE expectations were discarded from subsequent analyses with the exception of BayesAss, which does not require loci to be in HWE (Wilson & Rannala 2003). Loci deemed under selection were excluded from F_{ST} , Ima2 and demographic analyses, but not STRUCTURE and BayesAss as the assumptions of these assignment methods are not violated (Pritchard *et al.* 2000; Wilson & Rannala 2003).

Pairwise F_{ST} and R_{ST} analyses (the microsatellite equivalent of F_{ST} incorporating the SMM) were performed in Arlequin (10^5 permutations). Compound loci were excluded from the R_{ST} analyses, as motif repeat numbers are unknown. To test the number of distinct populations represented in this study for all three species, STRUCTURE 2.3.4 (Pritchard *et al.* 2000) was used with an admixture ancestry model and correlated allele frequencies with sample locations as priors. Analyses were based on a 2×10^5 step 'burn-in' with 2×10^6 MCMC steps. Five replicates were run for each K (number of populations) from $K = 1$ to 5. The best K was determined by using the median $\ln(\text{Pr}(X|K))$ values to calculate $\text{Pr}(K=k)$ as suggested by the software developers (Pritchard *et al.* 2000) in combination with the ΔK method of Evanno *et al.* (2005). Best K was calculated using the CLUMPAK server (Kopelman *et al.* 2015).

276

277 Contemporary gene flow (within the last couple generations) between differentiated populations (as
278 determined by F_{ST} , R_{ST} and STRUCTURE) was estimated with BayesAss 3.03 (Wilson & Rannala
279 2003), which uses an assignment method within a Bayesian MCMC framework to estimate the
280 fraction of immigrants in a population. Three runs, each with 2×10^7 iterations and a 'burn-in' of $2 \times$
281 10^6 were performed with different random number seeds, with the average taken. DeltaA, DeltaF and
282 DeltaM were set to 0.2, 0.35 and 0.15 respectively. Long-term bi-directional gene flow between
283 differentiated populations in the form of M , the mutation rate-scaled per generation immigration rate
284 going back to the coalescent, was estimated with IMa2 using an isolation-with-migration model of an
285 ancestral population splitting in two with subsequent migration (Hey 2010) on a combined COI and
286 microsatellite dataset. In addition to M , IMa2 estimates the mutation-rate scaled effective population
287 size (θ) of the sampled and ancestral populations as well as the splitting time, τ . Initial short IMa2
288 runs were performed to optimize model parameters and find reasonable priors for MCMC search
289 efficiency. The following uniform prior limits were used in final runs: $\theta = 150$, $M = 5$, and $\tau = 10$.
290 Eighteen independent analyses (using random number seeds), each with 100 geometrically heated
291 chains, were run for 2×10^6 steps (genealogy sampling every 100 steps, yielding 2×10^4 trees) with the
292 length of 'burn-in' determined by the scrutiny of trend plots printed every six hours. Final burn-in
293 lengths for the runs were $\sim 1.5 \times 10^6$ steps per independent run. Final run trend plots were assessed to
294 ensure that results were consistent between runs. The maximum of 3×10^5 sampled genealogies were
295 then combined in L-mode and the significance of inferred immigration rates tested using likelihood-
296 ratio tests (LLR) (Nielsen & Wakeley 2001).

297

298 BOTTLENECK 1.2.2 (Cornuet & Luikart 1996) was used to test for recent bottlenecks or phases of
299 expansion, by assessing the mismatch between expected heterozygosities estimated from the allele
300 frequencies (H_e) and heterozygosities estimated from the number and spread of alleles (H_{eq}) based on
301 the assumption of mutation-drift equilibrium and a specific mutational model. Two models were used

(10⁴ permutations): the SMM and the Two Phase Model (TPM) incorporating 5% IAM, which has been shown to be closer to real world observations of microsatellite evolution (Di Rienzo *et al.* 1994). Compound loci were discarded for these analyses as the SMM requires the motif repeat number to be known.

Results

Population Diversity and Structure

79 COI haplotypes from a 642 bp alignment were recovered from 90 *Kiwa tyleri* individuals across the ESR. Consequently, haplotype diversity (*h*) was very high; 0.998 both at E2 and E9. *h* values from a 437 bp alignment of 84 *Gigantopelta chessoia* individuals (24 haplotypes) were lower with 0.865 and 0.855 at E2 and E9 respectively. For a 618 bp alignment of *Lepetodrilus* sp., 36 haplotypes accounted for the diversity of 140 individuals across E2, E9 and Kemp with *h* values of 0.614, 0.743 and 0.85 for E2, E9 and Kemp respectively (Table 2). There was no evidence for population differentiation with the COI dataset between E2 and E9 for all three species in this study, although there was strong evidence for a divergence between the ESR and Kemp limpet populations, with $F_{ST} > 0.45$ (Table 3) and few haplotypes shared between the ESR and Kemp (Fig. 2). All substitutions between the ESR and Kemp limpets were third codon synonymous substitutions. All but four individuals at Kemp (F622_3, F622_19, F622_26, F622_28) shared an A-G substitution at COI alignment position 87 that was exclusive to Kemp.

Microsatellite re-genotyping of 24 individuals from Roterman *et al.* (2013a) revealed mean error rates of 2.3%, 3.1% and 2.9% for *Kiwa tyleri*, *Gigantopelta chessoia* and *Lepetodrilus* sp. respectively. In total, 35 microsatellite loci were amplified: nine for *Kiwa tyleri* (one compound locus), 12 for *Gigantopelta chessoia* (two compound loci) and 14 for *Lepetodrilus* sp.. Observed heterozygosity was

slightly lower than expected heterozygosity for all species and sites and allelic richness values were similar at the two ESR locations. Kemp limpet allelic richness was lower than on the ESR sites (Table 2). No loci were linked according to LD pairwise tests and only one locus, LepESR_06, significantly deviated from HWE with heterozygote deficiency (Table S3, Supplementary Materials) after correction for multiple tests, where null alleles were also detected with MicroChecker. No selection was detected with *Kiwa tyleri* and *Gigantopelta chessoia*, however, four *Lepetodrilus* sp. loci were found to be under balancing selection (LepESR_02, LepESR_05, LepESR_07 and LepESR_14) and one under directional selection (LepESR_10). Additionally, under the SMM, another locus was found to be under directional selection (LepESR_11) (Table S4, Supplementary Materials).

Pairwise R_{ST} analyses revealed no pattern of microsatellite differentiation on the ESR for all three species (Table 3). However, significant differentiation was detected between Kemp and ESR lepetodrilids with R_{ST} values in excess of 0.29 (with similar F_{ST} values; Table S5, Supplementary Materials). Structure analyses (Table S6, Supplementary Materials) supported this finding for the limpets: both the ΔK method of Evanno *et al.* (2005) and the method using the median $\ln(\Pr(X|K))$ values to calculate $\Pr(K=k)$ (Pritchard *et al.* 2000) determined $K = 2$ to be the best number of populations, with ESR individuals belonging to one population (Fig. 3). For the kiwaides and peltospirids, the Pritchard *et al.* (2000) method supported $K = 1$, echoing the pairwise R_{ST} results. However, the ΔK method, which cannot detect the best K if $K = 1$ (Evanno *et al.* 2005), supported $K = 2$ along the ESR. Examination of STRUCTURE bar plots showing the estimated membership coefficients for each individual under the $K = 2$ model revealed no pattern between E2 and E9 with all individuals assigned equally to both populations (Fig. S2, Supplementary Materials). Consequently, the $K = 2$ estimate according to the ΔK method was rejected in favour of $K = 1$ for *Kiwa tyleri* and *Gigantopelta chessoia*.

Gene flow estimates

Estimates of gene flow were only conducted between ESR and Kemp limpets owing to a lack of differentiation for all three species on the ESR. BayesAss analyses revealed the contemporary per generation ESR-to-Kemp mean immigration rate was 0.028, whereas the Kemp-ESR immigration rate was 0.004 (Table S7, Supplementary Materials). The individual assignments indicated that individuals F622_3, F622_19 and F622_28 may be first generation migrants from the ESR (mean posterior probabilities of 0.81, 0.96 and 0.88 respectively) (Table S8, Supplementary Materials). In IMA2 analyses (seven microsatellite loci plus COI), the *Lepetodrilus* sp. COI substitution rate used for calibrating the analyses was based on the divergence (8.17 %) of *L. pustulosus* across the Easter Microplate, which formed 3.86 Ma (2.47-5.25 Ma) (Naar & Hey 1991; Rusby & Searle 1995) giving a mean rate of 6.40415×10^{-6} (4.70857×10^{-6} – 1.00081×10^{-5}) substitutions per gene per year. Trace outputs did not reveal any trends and estimated parameters were unimodal (Fig. 4). θ for the ancestral population as well as splitting time did not reach zero at the upper prior boundary and therefore the mean and the highest posterior density interval may be unrepresentative (Fig. 4). Under the isolation with migration model, the ESR limpet population is inferred to be roughly five times larger than the Kemp population, though both populations are far smaller than the ancestral population (Table 4) since splitting from each other 1.68 Ma (0.36-7.26 Ma, 95% HPD). According to LLR tests, Kemp-to-ESR immigration rates (going forwards in time) were non-significant, but ESR-to-Kemp rates were highly significant ($P < 0.001$) (Table 4) indicating long-term easterly gene flow since the splitting event.

Demography

With the COI dataset, Fu's F_s were significantly negative for all species at all locations consistent with either a recent demographic expansion following a bottleneck, or a selective sweep. Mismatch distributions were largely unimodal for all three species at all locations (Fig. S1, Supplementary

Materials). Hri scores for all species were non-significant; signifying exponential population expansion cannot be rejected. For the limpet and the peltospirid, median-joining networks revealed a distinctive star-like pattern (Fig. 2). A similar pattern was also noticeable with the kiwaid, however the number of equally parsimonious connections was too great for visualisation and one of several equally parsimonious trees was presented instead (Fig. 2). BSP plots for all three species (Fig. 2) modelled a pattern of demographic expansion within the last million years. *Kiwa tyleri* underwent demographic expansion ~500 Ka, with the peltospirid population expanding more recently at ~90 Ka. The Kemp limpets expanded ~130 Ka and the ESR population, ~50 Ka. Microsatellite BOTTLENECK analyses revealed a significant ($P < 0.05$) pattern of heterozygote deficiency relative to the heterozygosity estimated from the number and spread of alleles (H_{eq}) under SMM, for all three species (Table S9, Supplementary Materials), consistent with recent demographic expansion (Cornuet & Luikart 1996), although $H_{eq} > H_e$ was not significant for the peltospirid under the TPM.

Discussion

ESR Connectivity

Both COI and microsatellite datasets reveal no differentiation for all three species across ~440 km of the ESR. These results are comparable to levels of differentiation found at similar scales on the EPR (Plouviez *et al.* 2009; Coykendall *et al.* 2011), although the ESR may have a lower density of vent fields in comparison (Livermore 2006). The absence of differentiation is consistent with either panmixia, or range expansions so recent as to have left no signature in the diversity of mtDNA haplotypes. This study, then, finds no correlation between dispersal strategy and patterns of population structure on the ESR. Although all the study species appear to produce lecithotrophic larvae, the kiwaid mode of larval development is so abbreviated as to be nearly direct, with large, passive larvae expected to have a very limited dispersal capability (Thatje *et al.* 2015b), making an absence of kiwaid

population structure still surprising. These results, therefore augment a body of evidence that so far has failed to show a particularly strong correlation between dispersal strategy and patterns of population structure in the marine environment, and particularly in the deep sea (Creasey & Rogers 1999; Weersing & Toonen 2009; Vrijenhoek 2010; Selkoe & Toonen 2011; Faurby & Barber 2012; Mercier *et al.* 2013).

One factor that may help explain the unexpected absence of population structure in *K. tyleri* is the temperature regime of the Southern Ocean. Bottom temperatures encountered at the ESR were -1.3–0 °C (Rogers *et al.* 2012) and such low temperatures may boost lecithotrophic larval longevity by substantially slowing metabolic rate and arresting development, as has been shown for the larvae of the vent polychaete *Alvinella pompejana* at 2 °C (Pradillon *et al.* 2001). Antarctic conditions could conceivably allow kiwaid larvae to survive for several years, as has been shown with echinoderm lecithotrophic larvae in laboratory conditions (Shilling & Manahan 1994). At such low temperatures, dispersal strategy may have little or no effect on PLD, in keeping with the findings of Mercier *et al.* (2013) on echinoderms from high latitudes. *K. tyleri* may have a dispersal strategy optimised for retention, justifying high maternal investment in individual offspring, where the low temperature of the Scotia Sea substantially extends the ‘tail’ on the dispersal kernel distribution, therefore facilitating inter-patch connectivity along the ESR.

Additionally, the density of vent fields and hence, potential dispersal stepping stones along the ESR may be higher than is presently thought, facilitating dispersal. The detection of a hydrothermal plume on the deeper E5 segment (Fig. 1B) (Baker *et al.* 2005; Livermore 2006) raises the possibility that other vent fields may yet be discovered on the E3-E8 segments in future surveys. Nevertheless, a higher density of vent fields along the ESR would still present a dispersal challenge for *K. tyleri* as non-swimming, demersal larvae would need to overcome the huge depth disparity between the E2 and E9 segments and the deep axial valleys of E3-E8. Higher vent density alone may therefore be

insufficient in accounting for apparent kiwaid panmixia on the ESR, without considering the effect of temperature-enhanced dispersal.

Kemp Caldera

Despite no evidence of differentiation along the ESR, limpet COI and microsatellite datasets revealed high levels of differentiation between the ESR and Kemp, which are only ~95 km apart. This level of differentiation could reflect the ~1000 m depth disparity between the sites (~1600 m if the caldera rim is included). Differentiation across isobaths has been observed in both vent and non-vent deep-sea fauna owing to either limited vertical migration of larvae, or adaptive divergence across depth gradients, such as pressure, temperature, salinity or food availability (e.g. France & Kocher 1996; Etter *et al.* 1999; Cho & Shank 2010; Vrijenhoek 2010; Quattrini *et al.* 2015). The absence of *Kiwa tyleri* and *Gigantopelta chessoia* from Kemp may be a consequence of this depth disparity, if their larvae cannot migrate as far vertically as the limpets, or the conditions at Kemp are beyond their physiological tolerances. Additionally, the greater range of habitats that host *Lepetodrilus* individuals (Johnson *et al.* 2008), may reflect their tolerance of a wider set of conditions (and therefore additional dispersal stepping stones) compared to the other study species.

The observation of corroded limpet shells at Kemp suggests that these limpets may be experiencing physiological stress in the highly acidic and sub-oxic conditions. ESR-Kemp differentiation between the sites could therefore be the result of different hydrothermal fluid chemistries imposing different selective regimes at the sites, although the depth disparity itself may be enough. Notably, STRUCTURE and BayesAss analyses assigned three Kemp limpets (6.5% of those sampled) to the same population as those on the ESR (Fig. 3 and Table S8, Supplementary Materials). Such a level of immigration in the long term would be expected to prevent divergence between populations (Wright 1943) in the absence of selection. The two populations may therefore be undergoing incipient

speciation, with each population being adapted to different hydrothermal fluid chemistries or other environmental conditions (e.g. temperature or pressure); hybrid offspring may be unviable, or ESR limpet adults are unable to produce eggs in the local conditions, for example. The fact that nearly half of the microsatellite loci of *Lepetodrilus* sp. were deemed under some form of selection by the F_{ST} outlier method (LOSITAN) supports this. Other (not mutually exclusive) possibilities include the caldera being a reproductive sink for limpet larvae coming from the ESR and another nearby population or that recent recolonization from these populations has occurred following defaunation after an eruption, with insufficient time for admixture (Cole *et al.* 2014). Future sampling of Kemp limpets, as well as the discovery and exploration of vents nearby, may provide a clearer picture. Additionally, the use of high throughput sequencing methods to generate genome-wide single nucleotide polymorphism datasets, such as restriction-site-associated DNA sequencing (RAD-seq) (e.g. Reitzel *et al.* 2013) offers the prospect of identifying specific genes that are experiencing selection, which may provide insights into the ways that different environmental conditions impact hydrothermal vent organisms surviving at physiological extremes. Furthermore, it has been suggested that comparing populations that are geographically close, but experiencing different environmental conditions (e.g. ESR and Kemp lepetodrilids) is the ideal way to use the F_{ST} outlier method to detect the effects of selection on population differentiation (Lotterhos & Whitlock 2015).

Limpet Gene Flow Estimates

The results of the IMA2 analysis revealed a pattern of unidirectional gene flow from the ESR to Kemp (going forwards in time) since the splitting of a hypothesized ancestral population during the Pliocene; similar to the BayesAss estimates indicating predominantly easterly contemporary gene flow. These gene flow estimates are consistent with inferences of broadly easterly current flow in the deep waters of the eastern Scotia Sea, (Orsi *et al.* 1999; Naveira-Garabato *et al.* 2002; Meredith *et al.* 2008) indicating that cross-axis currents may be common on portions of the ESR, as was observed on

the expedition JCR224 (Larter 2009). It should be noted, however, that the association between past and present current regimes and long and short-term gene flow is often unclear (Hellberg 2009). Additionally, the inferred splitting age produced in IMA2 should be treated with caution, as the substitution rate used is probably highly conservative; rapidly-evolving genes like COI are likely to be saturated when vicariance events are used in calibrating processes occurring on population genetics timescales. The true rate may therefore be as much as an order of magnitude faster (Ho *et al.* 2011) and the same goes for the BSP estimates of bottleneck ages discussed below.

Diversity and Demography

Significantly negative Fu's F_s , unimodal mismatch distributions and star-like haplotype networks in the COI dataset, along with the results of microsatellite BOTTLENECK analyses, are consistent with all three species having experienced recent demographic bottlenecks followed by population expansions. This pattern is nearly universal in vent-endemic fauna and may reflect the inherent demographic instability of vent metapopulations (Vrijenhoek 2010). Selective sweeps at the COI locus can also result in similar patterns, but studies combining mitochondrial and nuclear sequence datasets of vent-endemic species reveal similar patterns of diversity across all loci (Plouviez *et al.* 2010; Coykendall *et al.* 2011).

A notable feature of *Lepetodrilus* sp. is that the ESR sites have lower COI diversity, but higher microsatellite allelic richness than at Kemp, which could be indicative of a selective sweep at the COI locus on the ESR. Such a selective sweep on the mitochondrial locus could also account, through genetic hitching, for the absence of any ESR individuals with the A-G substitution at COI third codon position 87. Alternatively, the discrepancy between the limpet COI and microsatellite dataset may reflect the different mutation rates of mitochondrial and microsatellite DNA after a recent demographic bottleneck and subsequent expansion on the ESR. Regardless of the precise mechanism

responsible for this discrepancy, the combined limpet COI and microsatellite dataset in the IMA2 analyses infers a smaller effective population at Kemp compared with the ESR, which chimes with expectations. However, the high COI diversity of the Kemp limpets ($h = 0.85$) is not compatible with a population solely restricted to a single, volcanically active caldera. It appears more likely that the Kemp limpets comprise part of a population that extends beyond the boundary of the caldera, with the steep walls of the caldera not acting as a dispersal filter for the limpet larvae, which is consistent with there being a high percentage (6.5%) of possible immigrants from the ESR (see earlier).

If the COI locus does reflect demographic processes however, then the remarkably high COI diversity of the kiwaid and the lower diversity of the ESR limpets (peltospirids intermediate) does not reflect observations of numerical dominance at the ESR (Marsh *et al.* 2012). Bayesian Skyline Plots (BSPs, Fig. 2) indicate these species experienced bottlenecks at different times, unlike Plouviez *et al.* (2009), where COI bottlenecks across multiple co-occurring taxa on the East Pacific Rise (EPR) were attributed to a single past eruptive episode. Whilst the inferred bottleneck ages presented are likely highly conservative (Ho *et al.* 2011), in relative terms, if a single event was responsible for the ESR bottlenecks, limpet COI substitution rates would have to be roughly ten times slower than that of the kiwaid. Such a difference is far higher than the spectrum of substitution rates across invertebrate taxa separated by the final appearance of the Panama Isthmus (varying by a factor of ~ 3.3) (Lessios 2008), or across vent taxa separated by the subduction of the Pacific-Farallon ridge (~ 2.1) (Vrijenhoek 2013). Different bottleneck ages amongst these species, therefore, may reflect varying intrinsic demographic sensitivities to the stochastic birth and death of vent fields and changing hydrographic conditions along the ESR during the Plio-Pleistocene. High kiwaid genetic diversity could then signify a greater metapopulation resilience to such changes on the ESR.

These data, however, are a momentary snapshot of processes occurring over millennia, making it difficult to directly link a particular life history trait to patterns of COI diversity within the scope of

this study and as already mentioned, substitution rates generated from vicariance events should be treated with caution. Additionally, given that vent-endemic fauna may regularly experience physiological stress in the extreme hydrothermal conditions, selective sweeps at the mitochondrial locus may be far more common compared with the residents of other marine environments. Nevertheless, the very high COI haplotype diversity of *Kiwa tyleri* on the ESR is consistent with the maintenance of a large, relatively (by vent standards) stable population and is similar to the level of haplotype diversity (> 0.95) exhibited by the polychaete worm *Alvinella pompejana* that has high site occupancy along the East Pacific Rise (Vrijenhoek, 2010). It seems likely therefore that there may be more vent fields hosting *Kiwa tyleri* on the ESR than presently anticipated, which warrants further investigation.

Biogeographic implications

As already discussed, the temperature regime of the Scotia Sea may be key in facilitating dispersal along the ESR. This could especially be the case for kiwaidae, where in warmer waters, higher metabolic rates may substantially reduce their potential dispersal range; populations might be more fragmented and more vulnerable to extinction on stretches of mid-ocean ridge where vents are short-lived and large eruptive events are common. This may account for why kiwaidae have been found on the Pacific-Antarctic Ridge (Macpherson *et al.* 2005) and at the junction between the EPR and the Galapagos Rift (Wang *et al.* 2013), but not on the fast-spreading Southern EPR, where such conditions are thought to be common (Van Dover 2000).

The results of the *Lepetodrilus* sp. gene flow analyses, consistent with long-term easterly current flow may have implications for the diversity of vent fauna in the region. Populations of species producing small, buoyant larvae, such as those that produce planktotrophic larvae may be particularly vulnerable to demographic bottlenecks and extinction, if cross-axis currents dominate on isolated ridges such as

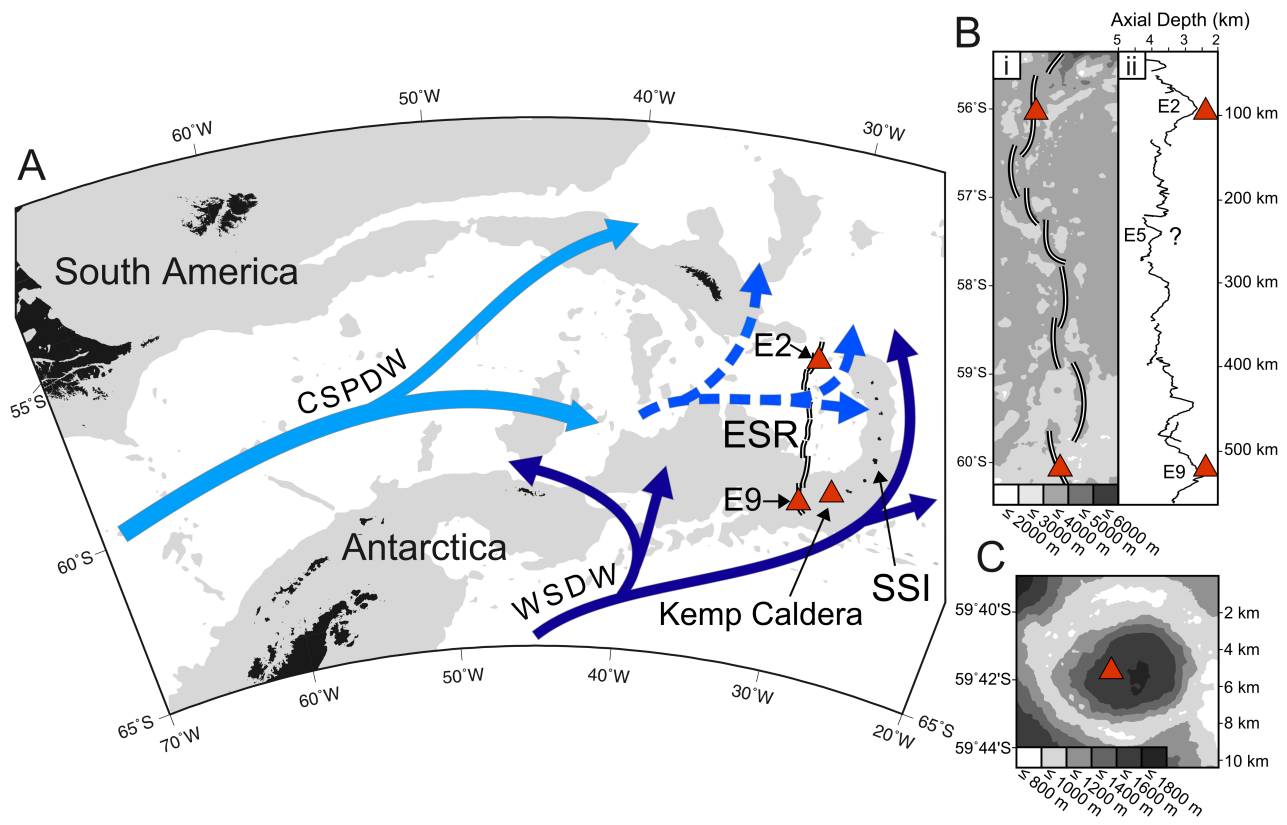
the ESR. The absence of planktotrophic species on the ESR as reported by Rogers *et al.* (2012), therefore, may have as much to do with the location and orientation of the ESR in relation to the ACC, as with the extreme seasonality of high latitudes (Pearse *et al.* 1991). If this is the case, then vent fauna producing planktotrophic larvae may yet be found in polar regions elsewhere. Given the risks of inferring currents from gene flow estimates mentioned earlier, however, only direct long-term current measurements on the ESR would reveal if cross-axis currents predominate.

A limitation of this study is its geographical extent, as well as the number of sites; constraining the number of inferences that can be made. The data presented here, however, represents the entire known range of the study species and should be seen as a primer for future population genetics studies of vent fauna in the Southern Ocean. Presently only two small vent regions have been explored in the Southern Ocean: the Scotia Sea and a segment of the Australian-Antarctic Ridge in the SW Pacific sector (Rogers *et al.* 2012; Hahm *et al.* 2015), despite the Southern Ocean being a biogeographical gateway to the other oceans of the world. This paucity of exploration and study reflects the challenges of operating research vessels and submersible craft in extreme polar conditions. The future sampling of vents on the American-Antarctic Ridge, in close proximity of the ESR and the southern part of the Southwest Indian and Mid-Atlantic Ridges, may yet provide greater insights into how the population structure and genetic diversity of the study species (or congeners) and other taxa are affected by intrinsic (e.g. life history, dispersal strategy) and extrinsic (e.g. temperature, the ACC, transform faults, current boundaries) factors in the Southern Ocean. The results will inform the ongoing debate regarding the impact of such intrinsic factors on population structure in the marine realm, with implications for the future management of marine resources.

585 **Acknowledgements**

586

587 Thanks goes to the JC042 expedition crews of RRS *James Cook* and ROV *ISIS* for collecting
588 specimens from vents in the most challenging conditions and to Dr Michelle Taylor and Dr Tom Hart
589 for their invaluable advice. Fieldwork and analyses were funded by NERC Consortium Grant
590 NE/DO1249X/1, NERC Grant NE/F005504/1 and NERC PhD studentship NE/D01429X/1(CNR,
591 JTC, KL, PAT, ADR).



593 Figure 1. A) Deep-water currents in the Scotia Sea, modified from other sources (Livermore 2006;
594 Orsi *et al.* 1999; Naveira-Garabato *et al.* 2002; Meredith *et al.* 2008). WSDW = Weddell Sea Deep
595 Water, CSPDW = Circumpolar and South Pacific Deep Water flow. Dashed arrow is a mixture of
596 WSDW and CSPDW. ESR = East Scotia Ridge, SSI = South Sandwich Islands. Areas shaded in light
597 grey are $\leq 3,000$ m depth. B) (i) Shaded bathymetric contour map of the ESR and (ii) depth profile of
598 the ESR axis, modified from other sources (Livermore 2006; Amon *et al.* 2013). ? = a detected
599 hydrothermal plume. C) Shaded bathymetric contour map of the Kemp Caldera, modified from Amon
600 *et al.* 2013. In all figure panels, triangles represent sampled hydrothermal vents. Double lines in A)
601 and B) (i) indicate actively-spreading ridge.
602

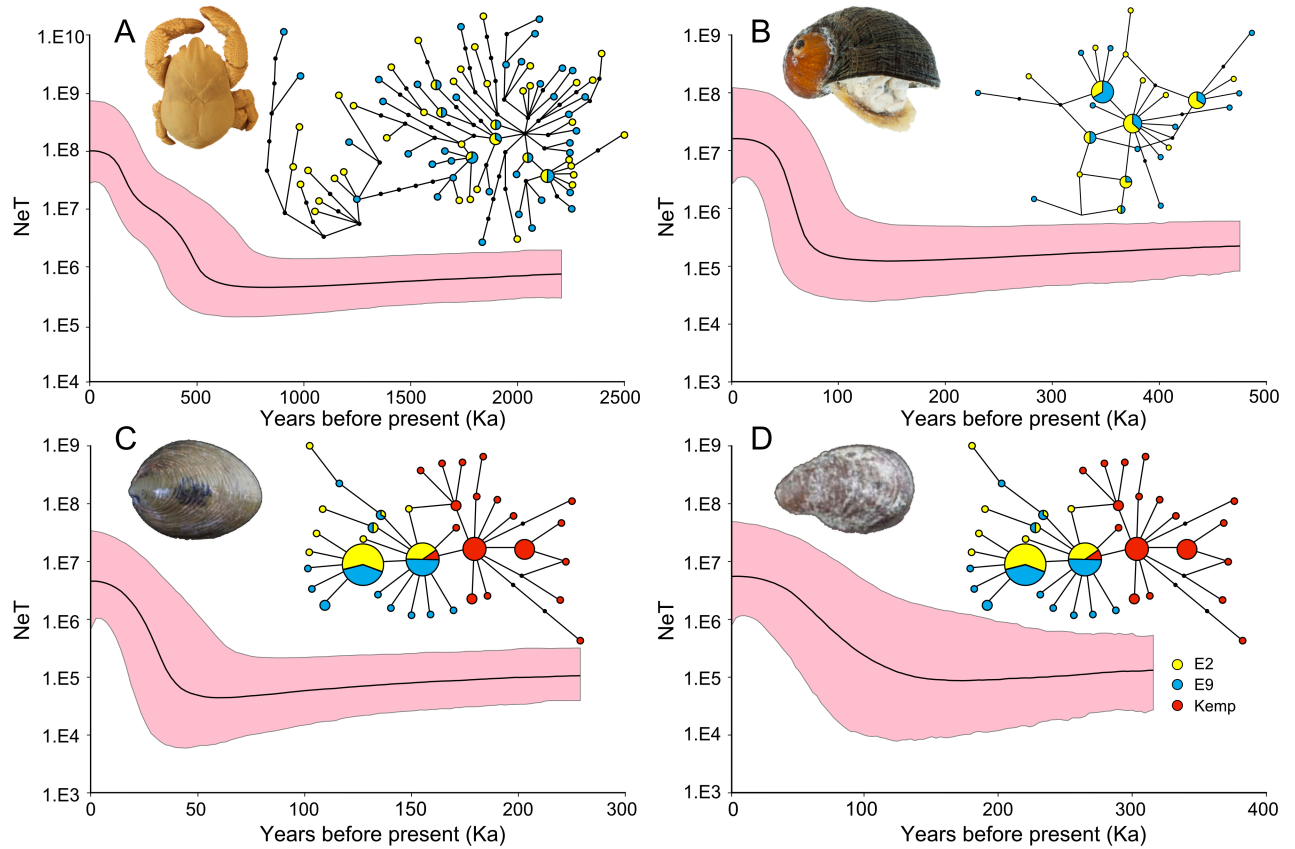


Figure 2. COI Bayesian skyline plots (BSPs) of (A) *Kiwa tyleri*, (B) *Gigantopelta chessoia*, (C) *Lepetodrilus* sp. collected from the E2 and E9 vent fields on the East Scotia Ridge and (D) *Lepetodrilus* sp. collected from the Kemp Caldera, with median-spanning haplotype networks (median spanning tree for *K. tyleri*) for each species. For the haplotype networks, circles represent haplotypes. Black circles denote hypothesised haplotypes. Lines represent base pair changes. Shaded circles are scaled to the number of individuals. For the BSPs, black lines denote median estimates with shaded areas representing 95% HPD intervals. Taxon-centric substitution rates (see text) were generated from the divergence of vent species either side of the Easter Microplate, which formed ~ 5.25 – 2.47 Ma (mean age of 3.86 Ma) (Naar & Hey 1991; Rusby & Searle 1995) on the Southern East Pacific Rise. Substitution rates were 9.45596×10^{-9} , 1.45078×10^{-8} and 1.0583×10^{-8} substitutions/locus/year for *K. tyleri*, *G. chessoia* and *Lepetodrilus* sp. respectively. NeT on the y-axis represents the generation time-scaled effective population size.

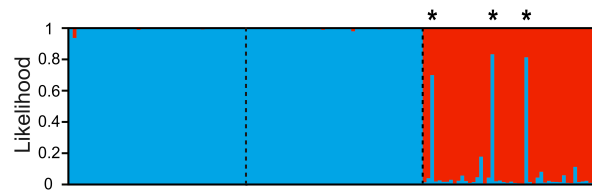


Figure 3. STRUCTURE individual assignment bar plots of *Lepetodrilus* sp. collected at hydrothermal vents on the East Scotia Ridge (ESR) at E2 and E9 and the Kemp Caldera, based on the two population model using 13 microsatellite loci. Three individuals, F622_3, F622_19 and F622_28 are marked (asterisk) as possible first generation migrants and exhibit ESR-like COI haplotypes.

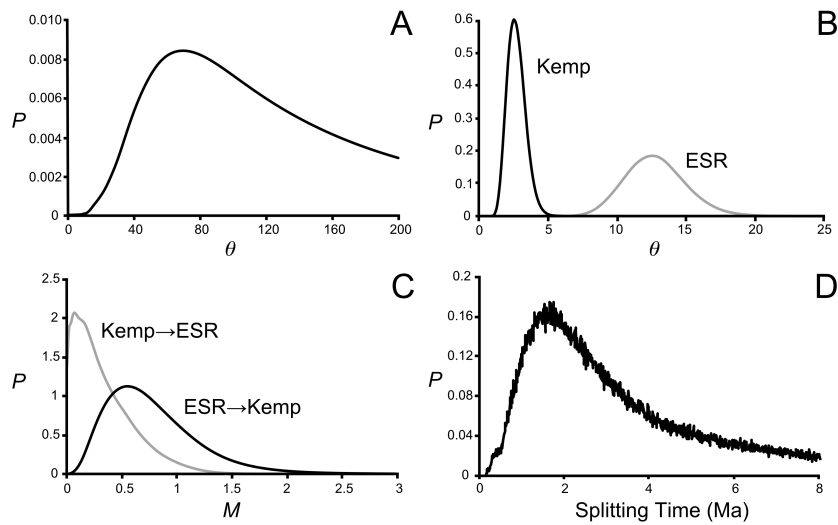


Figure 4. IMA2 gene flow output for *Lepetodrilus* sp. between hydrothermal vents on the East Scotia Ridge (ESR) and the Kemp Caldera using seven microsatellite loci and a 618 bp fragment of COI. Marginal posterior densities, P , of model parameters generated in L-mode (300,000 genealogies) showing (A) estimates of θ (mutation rate-scaled effective population size) for the ancestral population (B) estimates of θ of ESR and Kemp populations (C) immigration rates, M and (D) the estimate of the splitting time (in millions of years) of the ancestral population into the two populations. The analysis was calibrated by incorporating a COI substitution rate of 6.40415×10^{-6} substitutions/gene/year, based on the 8.17% divergence of *Lepetodrilus pustulosus* across the Easter Microplate (Johnson *et al.* 2008), which formed a mean age of 3.86 Ma (2.47-5.25 Ma) (Naar & Hey 1991; Rusby & Searle 1995).

Tables

Table 1. Sampling locations for the collection of *Kiwa tyleri*, *Gigantopelta chessoia*, *Lepetodrilus* sp. from hydrothermal vents on the East Scotia Ridge (ESR) and in the Kemp Caldera, South Sandwich Islands arc (SSI).

Species	Ridge/Arc	Segment/Caldera	Location	Date	Lat	Long	Depth (m)
<i>Kiwa tyleri</i>	ESR	E2	Crab City	25.01.2010	56° 05.345' S	30° 19.088' W	2,641
		E9	Black & White	30.01.2010	60° 02.564' S	29° 58.898' W	2,402
<i>Gigantopelta chessoia</i>	ESR	E2	Cinderella's Castle	24.01.2010	56° 05.359' S	30° 19.099' W	2,644
		E9	Marshland	30.01.2010	60° 02.807' S	29° 58.708' W	2,394
<i>Lepetodrilus</i> sp.	ESR	E2	Cinderella's Castle	24.01.2010	56° 05.359' S	30° 19.099' W	2,645
		E9	Marshland	02.02.2010	60° 02.800' S	29° 58.696' W	2,396
	SSI	Kemp	Winter Palace	09.02.2010	59° 41.695' S	28° 20.982' W	1,434

Table 2. COI and Microsatellite diversity indices for *Kiwa tyleri*, *Gigantopelta chessoia* and *Lepetodrilus* sp. sampled from hydrothermal vents on the East Scotia Ridge and the Kemp Caldera. For COI, sample size (n), number of haplotypes (Nh), haplotype diversity (h), nucleotide diversity (π), Fu's F_s are reported ($P < 0.05$, in bold). For the microsatellites (shaded), sample size (n), number of loci ($nLoci$), mean number of alleles (A), mean allelic richness (A_R), observed heterozygosity (H_{obs}) and expected heterozygosity (H_{exp}) are reported.

Species	Location	n	Size(bp)	Nh	h	π	F_s	n	$nLoci$	A	A_R	H_{exp}	H_{obs}
<i>Kiwa tyleri</i>	E2	45	642	43	0.998 (0.005)	0.0117	-24.97	46	9	11 (9.19)	10.94	0.65	0.62
	E9	45	642	43	0.998 (0.005)	0.0095	-25.25	45	9	10.11 (8.95)	10.11	0.63	0.62
<i>Gigantopelta chessoia</i>	E2	43	437	15	0.865 (0.030)	0.0044	-8.15	43	12	6.83 (5.10)	6.72	0.50	0.48
	E9	41	437	18	0.855 (0.044)	0.0051	-11.78	41	12	5.58 (4.03)	5.58	0.51	0.50
<i>Lepetodrilus</i> sp.	E2	47	618	10	0.614 (0.064)	0.0015	-5.93	47	14	12.86 (7.53)	12.79	0.69	0.65
	E9	47	618	13	0.743 (0.047)	0.0018	-9.48	47	14	13.07 (7.99)	12.93	0.68	0.66
	Kemp	46	618	19	0.850 (0.040)	0.0027	-16.18	46	14	8.50 (3.94)	8.50	0.63	0.62

Table 3. COI F_{ST} and microsatellite R_{ST} pairwise comparison matrix of *Kiwa tyleri*, *Gigantopelta chessoia* and *Lepetodrilus* sp., at hydrothermal vents on the East Scotia Ridge and the Kemp Caldera. R_{ST} values are shaded ($P < 0.05$ in bold).

Species		E2	E9	Kemp
<i>Kiwa tyleri</i>	E2	-	-0.008	-
	E9	0.002	-	-
<i>Gigantopelta chessoia</i>	E2	-	0.011	-
	E9	-0.006	-	-
<i>Lepetodrilus</i> sp.	E2	-	-0.006	0.293
	E9	0.003	-	0.323
	Kemp	0.496	0.454	-

Table 4. Summary results of IMA2 analyses (in L mode, 300,000 genealogies) on *Lepetodrilus* sp. from the East Scotia Ridge (ESR) and the Kemp Caldera in the Scotia Sea under a model of an ancestral population splitting with subsequent bidirectional gene flow. Parameter values are taken from estimated marginal posteriors. High Point values denoting peak values. HPD 95% values taken from the estimated 95% highest posterior density interval. Displayed estimated parameters are the mutation rate-scaled effective size of the populations (θ), the mutation rate-scaled per generation immigration rate, displayed going forwards from the coalescent (M), the mutation rate-scaled splitting time (τ) and the splitting time in years based on rate of a 6.40415×10^{-6} substitutions/gene/year. Likelihood-ratio tests (LLR) of immigration rates were either highly significant (***, $P < 0.001$) or not significant (^{ns}). [†] = upper marginal posterior bounds that did not reach zero at the upper prior boundary.

Parameter	High Point	Mean	HPD 95% Low	HPD 95% High
θ ESR	12.50	12.82	8.10	17.70
θ Kemp	2.50	2.70	1.10	4.90
θ Ancestral	70.10	102.10	31.70	192.3 [†]
M ESR→Kemp	0.55 ***	0.78	0.13	1.60
M Kemp→ESR	0.07 ^{ns}	0.33	0.0	0.85
τ	3.13	5.67	0.67	13.51 [†]
Splitting time (yrs)	1680633	3046842	358696	7258560 [†]

References

- Amon DJ, Glover AG, Wiklund H *et al.* (2013) The discovery of a natural whale fall in the Antarctic deep sea. *Deep Sea Research Part II: Topical Studies in Oceanography*, **92**, 87–96.
- Antao T, Lopes A, Lopes R, Beja-Pereira A, Luikart G (2008) LOSITAN: a workbench to detect molecular adaptation based on a Fst-outlier method. *BMC bioinformatics*, **9**, 323.
- Baker ET, Massoth GJ, Nakamura K-I *et al.* (2005) Hydrothermal activity on near-arc sections of back-arc ridges: results from the Mariana Trough and Lau Basin. *Geochem. Geophys. Geosyst.*, **6**.
- Bandelt H-J, Forster P, Röhl A (1999) Median-joining networks for inferring intraspecific phylogenies. *Molecular Biology and Evolution*, **16**, 37–48.
- Beaumont MA, Nichols RA (1996) Evaluating loci for use in the genetic analysis of population structure. *Proceedings of the Royal Society of London. Series B: Biological Sciences*, **263**, 1619–1626.
- Chen C, Copley JT, Linse K, Rogers AD (2015a) Low connectivity between “scaly-foot gastropod” (Mollusca: Peltospiridae) populations at hydrothermal vents on the Southwest Indian Ridge and the Central Indian Ridge. *Organisms Diversity & Evolution*, 1–8.
- Chen C, Linse K, Copley JT, Rogers AD (2015b) The “scaly-foot gastropod”: a new genus and species of hydrothermal vent-endemic gastropod (Neomphalina: Peltospiridae) from the Indian Ocean. *Journal of Molluscan Studies*, **81**, 322–334.
- Chen C, Linse K, Roterman CN, Copley JT, Rogers AD (2015c) A new genus of large hydrothermal vent-endemic gastropod (Neomphalina: Peltospiridae). *Zoological Journal of the Linnean Society*, **175**, 319–335.
- Cho W, Shank TM (2010) Incongruent patterns of genetic connectivity among four ophiuroid species with differing coral host specificity on North Atlantic seamounts. *Marine Ecology*, **31**, 121–143.
- Cole CS, James RH, Connelly DP, Hathorne EC (2014) Rare earth elements as indicators of hydrothermal processes within the East Scotia subduction zone system. *Geochimica et Cosmochimica Acta*, **140**, 20–38.
- Corliss JB, Dymond J, Gordon LI *et al.* (1979) Submarine thermal springs on the Galapagos Rift. *Science*, **203**, 1073–1083.
- Cornuet JM, Luikart G (1996) Description and power analysis of two tests for detecting recent population bottlenecks from allele frequency data. **144**, 2001–2014.
- Coykendall DK, Johnson SB, Karl SA, Lutz RA, Vrijenhoek RC (2011) Genetic diversity and demographic instability in *Riftia pachyptila* tubeworms from eastern Pacific hydrothermal vents. *Bmc Evolutionary Biology*, **11**, 96.
- Creasey SS, Rogers AD (1999) Population genetics of bathyal and abyssal organisms. *Advances in Marine Biology*, **35**, 1–151.
- Di Rienzo A, Peterson AC, Garza JC *et al.* (1994) Mutational processes of simple-sequence repeat loci in human populations. *Proceedings of the National Academy of Sciences*, **91**, 3166–3170.
- Drummond A, Rambaut A (2007) BEAST: Bayesian evolutionary analysis by sampling trees. *Bmc Evolutionary Biology*, **7**, 214.
- Etter RJ, Rex MA, Chase MC, Quattro JM (1999) A genetic dimension to deep-sea biodiversity. *Deep Sea Research Part I: Oceanographic Research Papers*, **46**, 1095–1099.
- Evanno G, Regnaut S, Goudet J (2005) Detecting the number of clusters of individuals using the software structure: a simulation study. *Molecular Ecology*, **14**, 2611–2620.
- Excoffier L, Lischer HEL (2010) Arlequin suite ver 3.5: a new series of programs to perform population genetics analyses under Linux and Windows. *Molecular Ecology Resources*, **10**, 564–567.
- Faurby S, Barber PH (2012) Theoretical limits to the correlation between pelagic larval duration and population genetic structure. *Molecular Ecology*, **21**, 3419–3432.
- Folmer O, Black M, Hoeh W, Lutz R, Vrijenhoek R (1994) DNA primers for amplification of mitochondrial cytochrome c oxidase subunit I from diverse metazoan invertebrates. *Molecular Marine Biology and Biotechnology*, **3**, 294–299.

- France SC, Kocher TD (1996) Geographic and bathymetric patterns of mitochondrial 16S rRNA sequence divergence among deep-sea amphipods, *Eurythenes gryllus*. *Marine Biology*, **126**, 633–643.
- Frederich M, Sartoris FJ, Portner HO (2001) Distribution patterns of decapod crustaceans in polar areas: a result of magnesium regulation? *Polar Biology*, **24**, 719–723.
- Fu YX (1996) New statistical tests of neutrality for DNA samples from a population. **143**, 557.
- Gage JD, Tyler PA (1992) *Deep-sea biology: a natural history of organisms at the deep-sea floor*. Cambridge University Press.
- Goudet J (1995) FSTAT (version 1.2): a computer program to calculate F-statistics. *Journal of Heredity*, **86**, 485–486.
- Guinot D, Hurtado LA (2003) Two new species of hydrothermal vent crabs of the genus *Bythograea* from the southern East Pacific Rise and from the Galapagos Rift (Crustacea Decapoda Brachyura Bythograeidae). *Comptes Rendus Biologies*, **326**, 423–439.
- Hahm D, Baker ET, Rhee TS *et al.* (2015) First hydrothermal discoveries on the Australian-Antarctic Ridge: Discharge sites, plume chemistry, and vent organisms. *Geochem. Geophys. Geosyst*, n/a–n/a.
- Hellberg ME (2009) Gene flow and isolation among populations of marine animals. *Annual Review of Ecology, Evolution, and Systematics*, **40**, 291–310.
- Hey J (2010) Isolation with migration models for more than two populations. *Molecular Biology and Evolution*, **27**, 905–920.
- Ho SYW, Shapiro B (2011) Skyline-plot methods for estimating demographic history from nucleotide sequences. *Molecular Ecology Resources*, **11**, 423–434.
- Ho SYW, Lanfear R, Bromham L *et al.* (2011) Time-dependent rates of molecular evolution. *Molecular Ecology*, **20**, 3087–3101.
- Jablonski D, Lutz RA (1983) Larval ecology of marine benthic invertebrates: paleobiological implications. *Biol. Rev.*, **58**, 21–89.
- Johnson SB, Warren A, Vrijenhoek RC (2008) DNA barcoding of *Lepetodrilus* limpets reveals cryptic species. *Journal of Shellfish Research*, **27**, 43–51.
- Jollivet D, Chevaldonne P, Planque B (1999) Hydrothermal-vent alvinellid polychaete dispersal in the eastern Pacific. 2. A metapopulation model based on habitat shifts. *Evolution*, **53**, 1128–1142.
- Kopelman NM, Mayzel J, Jakobsson M, Rosenberg NA, Mayrose I (2015) CLUMPAK: a program for identifying clustering modes and packaging population structure inferences across K. *Molecular Ecology Resources*.
- Lanfear R, Calcott B, Ho SYW, Guindon S (2012) PartitionFinder: combined selection of partitioning schemes and substitution models for phylogenetic analyses. *Molecular Biology and Evolution*, **29**, 1695–1701.
- Larter R (2009) *Cruise Report JR224. Chemosynthetically-driven ecosystems south of the polar front consortium programme. RRS James Clark Ross*.
- Leese F, Brand P, Rozenberg A *et al.* (2012) Exploring pandora's box: potential and pitfalls of low coverage genome surveys for evolutionary biology. *Plos One*, **7**, e49202.
- Lessios HA (2008) The Great American Schism: Divergence of Marine Organisms after the Rise of the Central American Isthmus. *Annual Review of Ecology, Evolution, and Systematics*, **39** IS -, 63–91.
- Livermore R (2006) The East Scotia Sea: mantle to microbe. *Geophysical monograph*, **166**, 243–261.
- Lotterhos KE, Whitlock MC (2015) The relative power of genome scans to detect local adaptation depends on sampling design and statistical method. *Molecular Ecology*, **24**, 1031–1046.
- Lutz RA, Bouchet P, Jablonski D, Turner RD, Warren A (1986) Larval ecology of mollusks at deep-sea hydrothermal vents. *American Malacological Bulletin*, **4**, 49–54.
- Macpherson E, Jones W, Segonzac M (2005) A new squat lobster family of Galatheaidea (Crustacea, Decapoda, Anomura) from the hydrothermal vents of the Pacific-Antarctic Ridge. *Zoosystema*, **27**, 709–723.
- Marsh L, Copley JT, Huvenne VAI *et al.* (2012) Microdistribution of faunal assemblages at deep-sea

- hydrothermal vents in the Southern Ocean. *Plos One*, **7**, e48348.
- Marsh L, Copley JT, Tyler P, Thatje S (2015) In hot and cold water: differential life-history traits are key to success in contrasting thermal deep-sea environments. *Journal of Animal Ecology*.
- Matabos M, Thiebaut E (2010) Reproductive biology of three hydrothermal vent peltospirid gastropods (*Nodopelta heminoda*, *N. subnoda* and *Peltoispira operculata*) associated with Pompeii worms on the East Pacific Rise. *Journal of Molluscan Studies*, **76**, 257–266.
- Matabos M, Plouviez S, Hourdez S *et al.* (2011) Faunal changes and geographic crypticism indicate the occurrence of a biogeographic transition zone along the southern East Pacific Rise. *Journal of Biogeography*, **38**, 575–594.
- Mercier A, Sewell MA, Hamel JF (2013) Pelagic propagule duration and developmental mode: reassessment of a fading link. *Global Ecology and Biogeography*, **22**, 517–530.
- Meredith MP, Garabato ACN, Gordon AL, Johnson GC (2008) Evolution of the deep and bottom waters of the Scotia Sea, Southern Ocean, during 1995–2005*. *Journal of Climate*, **21**, 3327–3343.
- Minin V, Abdo Z, Joyce P, Sullivan J (2003) Performance-based selection of likelihood models for phylogeny estimation. *Systematic Biology*, **52**, 674–683.
- Mullineaux LS, Mills SW, Sweetman AK *et al.* (2005) Vertical, lateral and temporal structure in larval distributions at hydrothermal vents. *Marine Ecology-Progress Series*, **293**, 1–16.
- Mullineaux LS, Wiebe PH, Baker ET (1995) Larvae of benthic invertebrates in hydrothermal vent plumes over Juan de Fuca Ridge. *Marine Biology*, **122**, 585–596.
- Naar DF, Hey RN (1991) Tectonic evolution of the Easter Microplate. *J. Geophys. Res.*, **96**, 7961–7993.
- Naveira-Garabato AC, Heywood KJ, Stevens DP (2002) Modification and pathways of Southern Ocean deep waters in the Scotia Sea. *Deep Sea Research Part I: Oceanographic Research Papers*, **49**, 681–705.
- Nielsen R, Wakeley J (2001) Distinguishing migration from isolation: a Markov chain Monte Carlo approach. *Genetics*, **158**, 885.
- Orsi AH, Johnson GC, Bullister JL (1999) Circulation, mixing, and production of Antarctic Bottom Water. *Progress In Oceanography*, **43**, 55–109.
- Pearse JS, McClintock JB, Bosch I (1991) Reproduction of Antarctic benthic marine invertebrates: tempos, modes, and timing. *American Zoologist*, **31**, 65–80.
- Pedersen RB, Rapp HT, Thorseth IH *et al.* (2010) Discovery of a black smoker vent field and vent fauna at the Arctic mid-ocean ridge. *Nature Communications*, **1**, 126.
- Plouviez S, Le Guen D, Lecompte O, Lallier FH, Jollivet D (2010) Determining gene flow and the influence of selection across the equatorial barrier of the East Pacific Rise in the tube-dwelling polychaete *Alvinella pompejana*. *Bmc Evolutionary Biology*, **10**, 220.
- Plouviez S, Schultz TF, McGinnis G *et al.* (2013) Genetic diversity of hydrothermal-vent barnacles in Manus Basin. *Deep Sea Research Part I: Oceanographic Research Papers*, **82**, 73–79.
- Plouviez S, Shank TM, Faure B *et al.* (2009) Comparative phylogeography among hydrothermal vent species along the East Pacific Rise reveals vicariant processes and population expansion in the South. *Molecular Ecology*, **18**, 3903–3917.
- Pradillon F, Shillito B, Young CM, Gaill F (2001) Deep-sea ecology: developmental arrest in vent worm embryos. *Nature*, **413**, 698–699.
- Pritchard JK, Stephens M, Donnelly P (2000) Inference of population structure using multilocus genotype data. *Genetics*, **155**, 945.
- Quattrini AM, Baums IB, Shank TM, Morrison CL, Cordes EE (2015) Testing the depth-differentiation hypothesis in a deepwater octocoral. *Proceedings of the Royal Society of London B: Biological Sciences*, **282**.
- Rambaut A, Drummond AJ (2007) Tracer v1. 4 [computer program]. Available at website <http://beast.bio.ed.ac.uk>.
- Reid WDK, Sweeting CJ, Wigham BD *et al.* (2013) Spatial differences in East Scotia Ridge hydrothermal vent food webs: influences of chemistry, microbiology and predation on

- trophodynamics. *Plos One*, **8**, e65553.
- Reitzel AM, Herrera S, Layden MJ, Martindale MQ, Shank TM (2013) Going where traditional markers have not gone before: utility of and promise for RAD sequencing in marine invertebrate phylogeography and population genomics. *Molecular Ecology*, **22**, 2953–2970.
- Rice WR (1989) Analyzing tables of statistical tests. *Evolution*, **43**, 223–225.
- Rogers AD (2010) *Chemosynthetic Ecosystems of the Southern Ocean (CHESSO)*. RRS James Cook Cruise 42.
- Rogers AD, Tyler PA, Connelly DP *et al.* (2012) The discovery of new deep-sea hydrothermal vent communities in the Southern Ocean and implications for biogeography. *Plos Biology*, **10**, e1001234.
- Rogers AR, Harpending H (1992) Population growth makes waves in the distribution of pairwise genetic differences. *Molecular Biology and Evolution*, **9**, 552.
- Roterman CN, Copley JT, Linse KT *et al.* (2013a) Development of polymorphic microsatellite loci for three species of vent-endemic megafauna from deep-sea hydrothermal vents in the Scotia Sea, Southern Ocean. *Conservation Genetics Resources*, **5**, 835–839.
- Roterman CN, Copley JT, Linse KT, Tyler PA, Rogers AD (2013b) The biogeography of the yeti crabs (Kiwaidae) with notes on the phylogeny of the Chirostyloidea (Decapoda: Anomura). *Proceedings. Biological sciences / The Royal Society*, **280**, 20130718–20130718.
- Rusby RI, Searle RC (1995) A history of the Easter microplate, 5.25 Ma to present. *J. Geophys. Res.*, **100**, 12617–12640.
- Schnabel KE, Ahyong ST (2011) A new classification of the Chirostyloidea (Crustacea: Decapoda: Anomura). *Zootaxa*, **2687**, 56–64.
- Selkoe KA, Toonen RJ (2011) Marine connectivity: a new look at pelagic larval duration and genetic metrics of dispersal. *Marine Ecology-Progress Series*, **436**, 291–305.
- Shilling FM, Manahan DT (1994) Energy metabolism and amino acid transport during early development of Antarctic and temperate echinoderms. *The Biological Bulletin*, **187**, 398–407.
- Teixeira S, Cambon Bonavita MA, Serrão EA, Desbruyeres D, Arnaud Haond S (2010) Recent population expansion and connectivity in the hydrothermal shrimp *Rimicaris exoculata* along the Mid-Atlantic Ridge. *Journal of Biogeography*, **38**, 564–574.
- Teixeira S, Serrão EA, Arnaud-Haond S (2012) Panmixia in a fragmented and unstable environment: the hydrothermal shrimp *Rimicaris exoculata* disperses extensively along the Mid-Atlantic Ridge. *Plos One*, **7**, e38521.
- Thaler AD, Plouviez S, Saleu W *et al.* (2014) Comparative Population Structure of Two Deep-Sea Hydrothermal-Vent-Associated Decapods (*Chorocaris* sp. 2 and *Munidopsis lauensis*) from Southwestern Pacific Back-Arc Basins. *Plos One*, **9**, e101345.
- Thaler AD, Zelnio K, Saleu W *et al.* (2011) The spatial scale of genetic subdivision in populations of *Ifremeria nautilei*, a hydrothermal-vent gastropod from the southwest Pacific. *Bmc Evolutionary Biology*, **11**, 372.
- Thatje S, Marsh L, Roterman CN, Mavrogordato MN, Linse K (2015a) Adaptations to Hydrothermal Vent Life in *Kiwa tyleri*, a New Species of Yeti Crab from the East Scotia Ridge, Antarctica (S Kiel, Ed.). *Plos One*, **10**, e0127621.
- Thatje S, Smith KE, Marsh L, Tyler PA (2015b) Evidence for abbreviated and lecithotrophic larval development in the yeti crab *Kiwa tyleri* from hydrothermal vents of the East Scotia Ridge, Southern Ocean. *Sexuality and Early Development in Aquatic Organisms*, **In Press**.
- Tyler PA, Young CM (2003) Dispersal at hydrothermal vents: a summary of recent progress. *Hydrobiologia*, **503**, 9–19.
- Tyler PA, Pendlebury S, Mills SW *et al.* (2008) Reproduction of gastropods from vents on the East Pacific Rise and the Mid-Atlantic Ridge. *Journal of Shellfish Research*, **27**, 107–118.
- Van Dover CL (2000) *The ecology of deep-sea hydrothermal vents*. Princeton University Press.
- van Oosterhout C, Hutchinson WF, Wills DP, Shipley P (2004) microchecker: software for identifying and correcting genotyping errors in microsatellite data. *Molecular Ecology Notes*, **4**, 535–538.
- Vrijenhoek RC (2013) On the instability and evolutionary age of deep-sea chemosynthetic

- communities. *Deep Sea Research Part II: Topical Studies in Oceanography*, **92**, 189–200.
- Vrijenhoek RC (1997) Gene flow and genetic diversity in naturally fragmented metapopulations of deep-sea hydrothermal vent animals. *Journal of Heredity*, **88**, 285–293.
- Vrijenhoek RC (2010) Genetic diversity and connectivity of deep-sea hydrothermal vent metapopulations. *Molecular Ecology*, **19**, 4391–4411.
- Wang J, Lin R, Bamber RN, Huang D (2013) Two new species of *Sericosura* Fry & Hedgpeth, 1969 (Arthropoda: Pycnogonida: Ammotheidae) from a hydrothermal vent on the East Pacific Rise. *Zootaxa*, **3669**, 165–171.
- Weersing K, Toonen RJ (2009) Population genetics, larval dispersal, and connectivity in marine systems. *Marine Ecology Progress Series*, **393**, 1–12.
- Wilson GA, Rannala B (2003) Bayesian inference of recent migration rates using multilocus genotypes. **163**, 1177–1191.
- Wright S (1943) Isolation by distance. **28**, 114.

889 **Data Accessibility**

890

891 COI sequences deposited in Genbank (Acc# KU312406 - KU312689).

892

893 Following data incorporated into a zip file called “Data_accessibility” - included in supplementary
894 section:

895

896 COI fasta files

897 Arlequin 3.5.1.3 input files

898 Beast 1.7.4 Bayesian Skyline Plot input xml files

899 Microsatellite genotype excel spreadsheets

900 STRUCTURE 2.3.4 input files and parameter files

901 BOTTLENECK 1.2.2 input files.

902 IMa2 input files.